RSC Advances

ROYAL SOCIETY OF CHEMISTRY

www.rsc.org/advances

Long-term Monitoring of Capase-3 Activity in Living Cells Based on the FRET Probe Composed of Quantum Dot, Nanogold and EGF

Dahai Ren*, Jun Wang, Zheng You

State Key Laboratory of Precision Measurement Technology and Instruments, Department of Precision Instrument, Tsinghua University, Beijing, 100084, China

Abstract: Conventional probes used to detect proteases are susceptible to either photobleaching or low efficiency in cell penetration. Also it is difficult to achieve multiplexed detection. Based on QD, nanogold and EGF, a unique probe was studied in the paper. The sensing section of the probe was developed by linking the streptavidin-labeled QD and monomaleimide-functionalized nanogold via a substrate peptide. The QD fluorescence is partially quenched by nanogold when they were connected. After the substrate peptide is cleaved by protease, the QD fluorescence can be partially recovered as the distance between two kinds of nanoparticles increases. Biotin-labeled EGF was used to carry the sensing section into the cells, making the transfection efficiency higher than former nanoprobes. After assays, we found the optimal ratios of nanogold to QD and to EGF to realize the high efficiency of both quenching and transfer. Also an algorithm was proposed to evaluate the relative activity of proteases. Finally, caspase-3 was used as the target protease to be detected. The activity of caspase-3 was successfully monitored during a longer time span compared to the reported probes.

Keywords: Quantum dot (QD); fluorescence resonance energy transfer(FRET); epidermal growth factor (EGF); multiplexed analysis; bio-MEMS

1. Introduction

Proteases perform essential functions in all living organisms and they are closely related to critical activities like cell-cycle regulation, immune and inflammatory cell migration, activation and apoptosis[1]. Caspases have been widely studied, as apoptosis is a vital cellular activity that plays a key role in pathogenic therapy for many diseases[2-4]. Among the spectrum of various caspases, caspase-3 is believed to be the primary executioner of apoptosis[3, 5].Traditionally, caspase activities are usually detected using western blot or membrane-impermeable fluorogenic enzyme substrates such as DEVD-R110. In these cases, cell lysis is required, and these detection methods are in vitro**.** In addition, these assays only measure the average activity of caspases in a highly heterogeneous cell population. However, cells within any given population are heterogeneous and undergo cellular processes such as apoptosis at different rates. Therefore, it is important to be able to detect these apoptotic events in individual living cells.

Fluorescence resonance energy transfer (FRET) probes composed of dual proteins or dual dyes[6-9] can be used to detect the activity of intracellular proteases like caspase-3. However, overlapping between the donor and accepter cannot be avoided and leads to low signal-to-noise ratios. Some cell penetrating single-color probes also occurred [10-13], but the weak resistance of photobleaching on these kinds of probes determines that all of them can only be observed for a limited time. Because of the excellent optical properties of quantum dots (QD), high quenching efficiency, and the outstanding bio-compatibility of nanogold, they have been employed respectively as donor[14, 15] and quencher[16, 17] to constitute FRET probes. This can avoid fluorescence overlapping and allow much longer detection time. However, unlike small molecules, the probes constituted by nanoparticles are unable to freely diffuse into the cells. As a result, the cell penetrating

efficiency of these probes is low[18-21].

Actually, the above mentioned FRET probes also cannot accurately reflect the activity of proteases as they may partially diffuse into the surrounding solution from the cytoplasm in a short time. This means that the measurement result derived from the fluorescence signal is not accurate. In 2008, Cen[22] synthesized a new probe consisting of a fluorogenic DNA dye (NucView488) and a DEVD substrate moiety specific tocaspase-3. The probe is both non-fluorescent and nonfunctional as a DNA dye, and can rapidly pass through cell membranes and enter the cytoplasm. This allows for the real-time detection of caspase-3 activities in live cells to some degree. However, it could not accurately reflect the activities of caspase-3, as not all the NucView488 are combined with the DNA. Also, like other dye-based probes, it is susceptible to severe photobleaching. To summarize, the reported probes are susceptible to either photobleaching or low efficiency in cell penetration, or both[23-26].

In this paper, based on the advantages of the reported probes, a new kind of probe was developed to overcome the above mentioned deficiencies. As shown in Figure1, the probe is composed of streptavidin-labeled QD, monomaleimide-functionalized nanogold, substrate peptide and biotin-labeled EGF. The substrate peptide mainly contains four functional sections: biotinylated N-terminal, C-terminal cysteine, protease recognition sequence and flanks. N-terminal biotin is used for coupling to the streptavidin-labeled QD. Cysteine at the C-terminal is used for coordinating coupling to a monomaleimide-functionalized nanogold. Protease recognition confirms the sub-peptide to be specifically cleaved by the corresponding protease. The function of the flanks is to decrease the steric hindrance and increase the chance that the recognition sequence can be cleaved.

The sensing section of the probe is developed by linking the streptavidin-labeled QD and monomaleimide-functionalized nanogold via a substrate peptide. When the distance between the QD and nanogold is short enough (less than 20nm), the QD fluorescence will be partially quenched by nanogold as a result of energy transfer or some other mechanisms. After the substrate peptide is cleaved by protease, the distance between the two kinds of nanoparticles would increase. As a result, the QD fluorescence can be partially recovered. Just like the substrate peptide, the biotin-labeled EGF also couples to the streptavidin-labeled QD. It can efficiently carry the sensing section into the cells by bonding with the EGFR[27, 28], which is ubiquitously expressed in normal cells and preferentially over-expressed on the surface of many cancer cells[29, 30].

Assembling this probe is simple. It can be used to detect intracellular proteases during a prolonged time span and give accurate results, and is a most promising probe that can be used in real-time monitoring of protease activity in living cells.

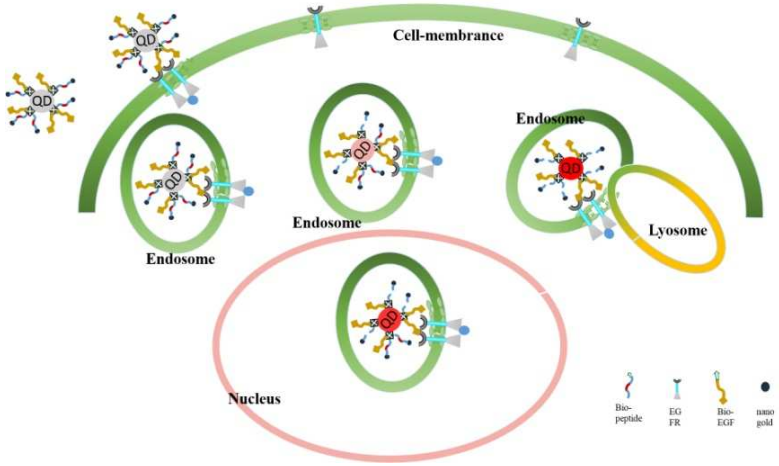

Figure1. Schematic Principle of Caspase-3 Detection in Living Cells with the EGF-QD-peptide-nanogold Probe

2. Experimental

2.1 Reagents and Apparatuses

Fetal bovine serum (FBS) (Gibco, USA), Phosphate buffer solution (PBS PH=7.4, 8.0), penicillin/streptomycin (Macgene, China), biotin-BSA (Gelest, USA), Streptavidin Alexa Fluor® 488 Conjugate(SA-Alex488) (Invitrogen, USA), 384-well and 96-well plates (Corning, USA), ultra-filter centrifuge tubes (Millipore, USA), microplate reader(PerkinElmer, Envision, USA). Confocal fluorescence microscope (A1RSi, Nikon, Japan), fluorescence microscope (IX71, Olympus, Japan), transmission electron microscopy (JEM 1200EX, Japan). Substrate peptide (subpeptide) (LifeTein, USA), Qdot605 streptavidin conjugates (SA-QD605) (Wu Han Jia Yuan, China), 1.4 Monomaleimido Nanogold (Nanoprobes, USA), Trypsin (Calbiochem, USA), TNF-α and AcD (Sigma, USA), Biotin-labeled EGF (Invitrogen, USA), Caspase-3 enzyme (Millipore, USA). Biotin-GRRG-DEVD-GGRRC was purchased from and was synthesized by standard automated Fmoc solid-phase peptide synthesis.

2.2 Probe Preparation

The sub-peptide was dissolved in PBS (PH=8.0) and the final concentration was 2nmol/μl. TCEP solution was prepared with the final concentration of 0.02M. 50μl sub-peptide (100nM) was pipetted into a 1.5ml tube and then diluted to 500μl by adding 450μl PBS. Then it was added into 2.5μl TCEP (100nM) and reacted for 30 minutes. This yielded a sub-peptide with reduced Cys[31,32]. 6nmol monomaleimide functionalized nanogolds (1.4 nm in diameter) were dissolved in 210μl double-distilled water.

70μl nanogolds solution (2nmol) was then pipetted and added into the 500μl reduced sub-peptide solution. The ratio of sub-peptide to nanogolds is about 50. The excess amount of peptide compared to the nanogold was used to ensure sufficient binding of the peptides to the nanogolds[15]. The resulting solution was incubated for 20hours at 4℃ without stirring.

After the reaction, the resulting solution was spin-filtered using a centrifugal filter (microcentricon, YM-10) with an exclusion cutoff of 10kDa to separate the unbound peptides from the Nanogold conjugates (Nanogold clusters typically have a molecular weight of 15kDa according to product specifications). Then, double-distilled water was added, and the solution was spin-filtered. The concentrated conjugates were resuspended in 335μl PBS and added into an appropriate quantity of BSA (the final concentration of BSA is 0.1%)[33]. The concentration of the conjugated nanogolds is 5pmol/μl, and is determined according to specifications in the manual. At this time, the nanogolds conjugated with the sub-peptides (sub-nanogold) were obtained and the resulting conjugates were stored at 4°C until use. As a control group, the remaining free nanogolds were reserved without any treatment.

The SA-QD605 was mixed with certain amounts of sub-nanogolds and biotinylated EGF in a 384-well plate for 30minutes at room temperature to allow specific association between SA and biotin[15].The ratios of EGF to QD and sub-nanogold to QD are about 3 and 12.5 respectively.

The final concentration of the probe in an aqueous solution was typically 5 nM (corresponding to 0.4 pmol in 80 μL reaction volume). The probe fluorescence intensity was measured at an excitation wavelength of 360 nm by using a microplate reader (Envision, PerkinElmer, USA).

2.3 Cell Culture

The human promyelocytic leukemia cell line HL-60 was maintained at the Roswell Park Memorial Institute (RPMI). The RPMI 1640 medium (Macgene, China) was supplemented with 10% FBS (Gibco, USA) and 1% penicillin/streptomycin solution. The cells were cultured in a humidified atmosphere at 37°C in 5% CO_2.

HeLa cells were cultured in Dulbecco's Modified Eagle's Medium (DMEM) (Macgene, China) and supplemented with 15% (vol/vol) FBS (Gibco, USA), and 1%penicillin/streptomycin solution. The cells were cultured in a humidified atmosphere of 5% (vol/vol) $CO_2$and 95% air (vol/vol) at 37 °C.

2.4 Cell Induction

HeLa and HL-60 cells were seeded in a 96-well plate, filled with 100μl completed culture medium. When the bottom of the plate was covered 60%-70%, cells needed to be induced were treated with TNF-α (the final concentration was 20 ng/ml), AcD (the final concentration was 0.2 μg/ml) and they were then incubated in a humidified atmosphere of 5% (vol/vol) $CO_2$and 95% air (vol/vol) at 37 °C[34-36].

2.5 Transfection of the Probes

Probes (the final concentration is 4nM) were incubated with HeLa cells in serum-free DMEM. After incubation for 2 hours, the probe containing serum-free DMEM was removed. Cells were washed with 200μlPBS three times and then supplemented with a 100μl culture medium. Subsequently, the cells were observed under the fluorescence microscope. The fluorescence of the probes can be excited efficiently by any wavelength from 300nm to 490nm. The central wavelength of the excitation used for our assays was 488nm. The emission wavelength of the probes was 605nm.

3. Results and Discussion

3.1 Characterization of the Probes

Assays were conducted to ascertain the optimal ratio of sub-nanogold to QD. A fixed amount of QD (80μl, 5nM) was added into varying amounts of sub-nanogold. Then we detected the fluorescence intensity (FI) of the reaction solution (Figure 2a).When the volume of sub-nanogold increases, the quenching effect of sub-nanogolds to the QDs also increases. However, when the volume of sub-nanogold surpasses 1μl, the degree of quenching does not clearly increase.

To determine the ideal concentration ratio of EGF to QD, we conducted assays on EGF-QD entering into cells. Similarly, fixed amounts of QD (0.4μl, 1μM) were mixed with varying amounts of EGF (0, 0.05μl, 0.1μl, 0.2μl, 0.3μl, 0.4μl, 0.6μl, 0.8μl, and 1μl). The EGF concentration was 6μM. The results showed that there was no clear difference in transfer efficiency when the amount of EGF was more than 0.2μl. To make sure that the QDs can, to a large degree, combine with and be quenched by nanogolds, in later assays, we fixed the ratio of EGF to QD as 3. According to the manual for the QDs, one QD is covered by 3 to 8 streptavidins. One streptavidin is able to be combined with 4 biotins on average. Therefore, in theory one QD can combine 12 to 32 biotins, namely 1pmol (1μl) QDs which can fully react with 22pmol biotins. Given steric hindrance, the actual number may be less than 22, and 0.4μl QD (1μM) can still fully react with 1.52μl sub-nanogold (5μM). Actually, 0.5μl of nanogold is enough to quench 0.4μl QD. The quenching efficiency of nanogold to QD did not change greatly when 0.2μl EGF was added (Figure 2b).

Comprehensively considering the quenching efficiency, the transfection efficiency and the reagent saving, we constructed the probes by mixing 0.4μl QD (1μM) with 0.2μlEGF (12μM) and 1μl nanogold-sub (5μM). Specifically, the ratios of EGF to QD and sub-nanogold to QD are about 3 and 12.5 respectively. The probe solution was stored at 4°C until use.

To confirm that the free nanogold will not quench the QD fluorescence, we mixed an appropriate amount of QD with varying amounts of free nanogold (Figure 2c). There was negligible change in the fluorescence intensity of the QD solution after 1μl, 6μM pure nanogold was added. Therefore, the effect of free nanogold on QD fluorescence can be ignored.

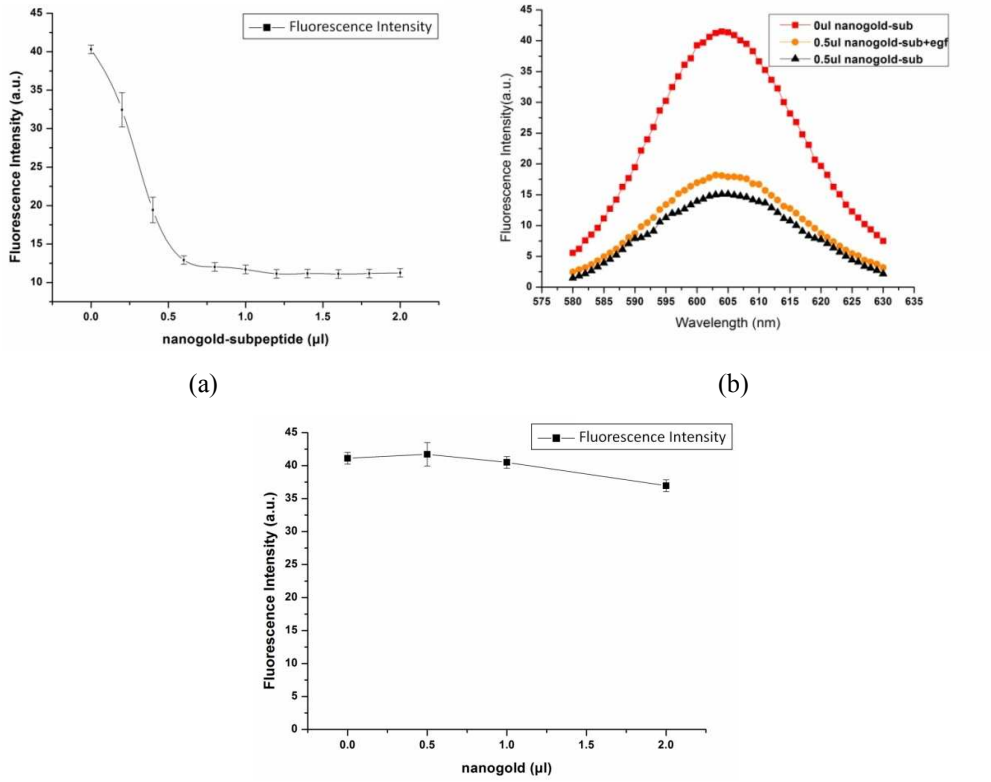

Figure 2. Measurement of the quenching efficiency of sub-nanogold (5μM) and free nanogold (6μM) to QD. (a) The quenching of nanogold-sub-peptide to QD is obvious. However, when the volume of sub-nanogold surpasses 1μl, the degree of quenching barely increases. (b) Adding EGF has a little effect on the quenching efficiency of nanogold to QD. There is no emission peak red-shift of QD. (c) Negligible change in the QD solution's FI after varying amounts of pure nanogold were added. The data is from five independent experiments.

We also further confirmed that the quenching of nanogold to QD required participation of biotin at the N-terminal of a substrate peptide. Before adding the nanogold-substrate peptide conjugate into the QD solution, first we added superfluous free biotin into the streptavidin-QD solution, and then found that the QD's FI would not be quenched by the sub-nanogold again, fitting the reported result[37].

The nanoparticles and probe were also characterized by TEM (Figure 3). As shown in Figure 3b, QDs were successfully conjugated to nanogolds.

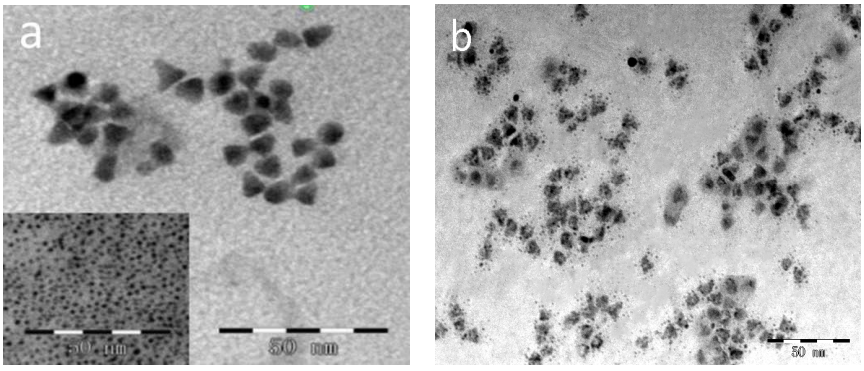

Figure 3. TEM images of nanoparticles and probes. (a) The image of SA-QD and nanogold. The insert is a nanogold image. (b) Probe image. The nanogolds are around the QDs. Transmission electron microscopy (TEM) images were obtained on a JEM 1200EX.

3.2 Detection of Caspase-3 Activity in Vitro

First, we reconstituted the caspase-3 to 1 unit/μl with PBS containing 15% glycerol. We pipetted 1μl caspase-3 (1 unit/μl) into 499μl PBS(PH=7.4). The concentration of diluted caspase-3 was 2 unit/ml. Then we mixed varying volumes (0.5μl, 1μl, 1.5μl, 2μl) of diluted caspase-3 with a 0.15μl probe(1μM), and added an appropriate volume of PBS (PH=7.4) to keep the final volume of reaction solution to 80μl. The assays were conducted in wells with a 384-well micro plate at 37°C. The fluorescence intensity of the enzymatic reaction solutions was measured by a fluorescence reader (VARIOSKAN FLASH, Thermo Scientific) at appropriate intervals (Figure 4). In the control group, the diluted caspase-3 was incubated with AC-DEVD-CHO before mixing with probe. The FI of 0.15μl pure QD was employed as a contrast.

As shown in Figure 4, without caspase-3, the probe's FI was stable in the buffer solution, showing negligible fluorescence signal change within 90minutes. The FI of the pure QD was the same. After adding caspase-3, an approximately 3-fold increase in the fluorescence intensity of the probe was observed. Since the fluorescence recovery was efficiently blocked in the control group by the adding caspase-3 inhibitor, we concluded that the increase in the fluorescence intensity of probes was caspase-3-specific.

The results showed that the probe fluorescence could be recovered by caspase-3. According to the control group, the probe fluorescence did not increase obviously, indicating that the activity of caspase-3 was effectively inhibited by the AC-DEVD-CHO and the recovery of fluorescence should be credited to caspase-3. However, recovery efficiency was not 100%, even though the probe was incubated with superfluous caspase-3. We presumed that this resulted from steric hindrance, namely that not all of the cleavable sites of the substrate peptides was accessible to caspase-3. Then, we conducted assays to confirm. First, we mixed the caspase-3 with the sub-nanogold, and the resulting solution was added with QD. The fluorescence intensity (FI) of this mixture was the same as that of the pure QD, even stronger (Figure 5). The stronger FI may also result from the biotin at the substrate peptide. In any case, the result confirmed that the large QD size would hinder the cleavage of caspase-3 to the substrate peptide.

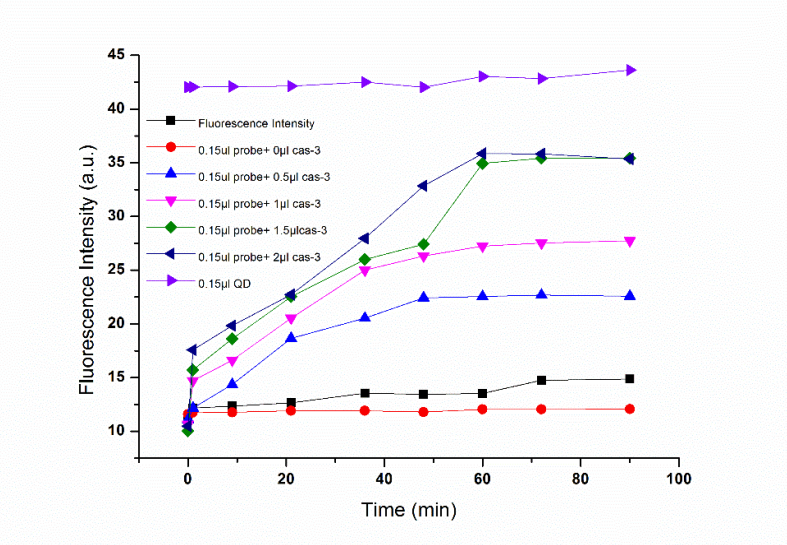

Figure 4. The change in the fluorescence intensity of the probe incubated with varying volume of caspase-3 (0, 0.5, 1, 1.5, 2μl). The FI of the probe, QD, and the control group were stable during the observation period.

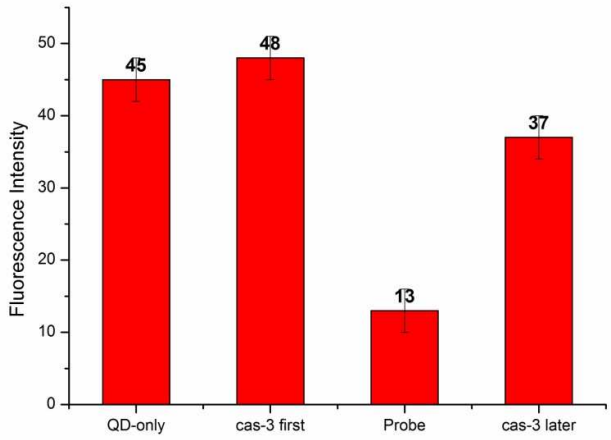

Figure 5. The column of "Only QD" represents the QD FI. Cas-3 first represents the FI of the resulting solution that incubated the sub-nanogold with superfluous caspase-3 before reacting with QD. The "Probe" denotes its FI. Cas-3 later denotes the FI of the resulting solution of the incubating probe with superfluous caspase-3.

3.3 Evaluation of EGF Transfection Efficiency

About 5×10^4 cells were seeded into three groups of wells in a 96-well plate, and were designated as A (without QD and EGF), B(with only QD) and C(with QD and EGF). In microcentrifuge tube C, we mixed 0.4μl QD and 0.2μl EGF in 20μl serum-free DMEM, allowing them to react for 30minutes, and then added 80μl serum-free DMEM. We also added 100μl serum-free DMEM into microcentrifuge tubes A and B, and added 0.4μl QD into tube B. Furthermore, we replaced the culture medium in the wells of A, B and C with the solution in the microcentrifuge tubes for A, B and C. It was repeated for all groups three times. Finally, we incubated the 96-well plate in the incubator for 2 hours, and all groups were observed by the fluorescence microscope (Figure 6).

We could observe obvious intracellular fluorescence in group C (Figure 6c) and all the cells were stained with red fluorescence. However, no red fluorescence could be observed in group A (Figure 6a), and only weak fluorescence in several cells could be observed in group B (Figure 6b).

Cell nucleus dyeing was employed to test whether EGF can bring quantum dots into the nucleus of cells. QD positions were observed with a confocal fluorescence microscope. Figures 6(d), 6(e) and 6(f) show the fluorescence locations at the nucleus which was stained with hochst33342, indicating that EGF carried QDs into the cell nucleus. As a result, it is difficult for QDs to diffuse into the surrounding solution from the cytoplasm in a short time. As mentioned in "Introduction", diffusion into the surrounding solution from the cytoplasm is a disadvantage of reported probes. These results show that EGF is an ideal candidate for carrying nanoparticles into the cells.

Furthermore, we employed the anti-EGFR to occupy the EGFR before adding a probe, and we found that the efficiency of transfection became lower compared to not adding anti-EGFR. It was confirmed that the probe was carried into cells by EGF[32].

According to our assays, most of the probes entered into the nucleus after one and a half hour (figure 6), if TNF-α and AcD was not added. However, if TNF-α and AcD were added into the culture medium about ten minutes after the probes was added, most of the probes would not enter into the nucleus (can be seen in figure 12). This can be explained by the fact that apoptosis of cell would decrease the rate of material transport.

As the probes are modified with EGF , they will enter into the endosome. It is hard to confirm that all the probes would be released from endosome. However, a portion of the probes would certainly be released, as the endosome would finally be melted by the lysosome. Particularly, the function of lysosome will increase when apoptosis happens. Therefore, (when cells are killed) the probes are able to characterize the activity of caspase-3 not only in endosome.

Another characteristic of the probes should be noted is that the probes will activate EGF signaling pathways and activate the receptor tyrosine kinase pathway. However, it will not negatively affect the working of the probes. First of all, the activity of tyrosine kinase pathway is not necessarily related to the activity of caspase-3. Besides, to some degree, the toxicity of nanoparticles or dyes could be decreased by EGF which will improve the activity of cells. We culture the cells with the probes for days, and cells could grow normally before induction. However, the growth of cells would be affected if cells were cultured with nanoparticles without modification by EGF or cultured with dyes. For example, their growth rate became slower and their shapes became abnormal. Because normal cell growth is preserved, the using of EGF could not be regarded as disadvantage, but, to some degree, advantage.

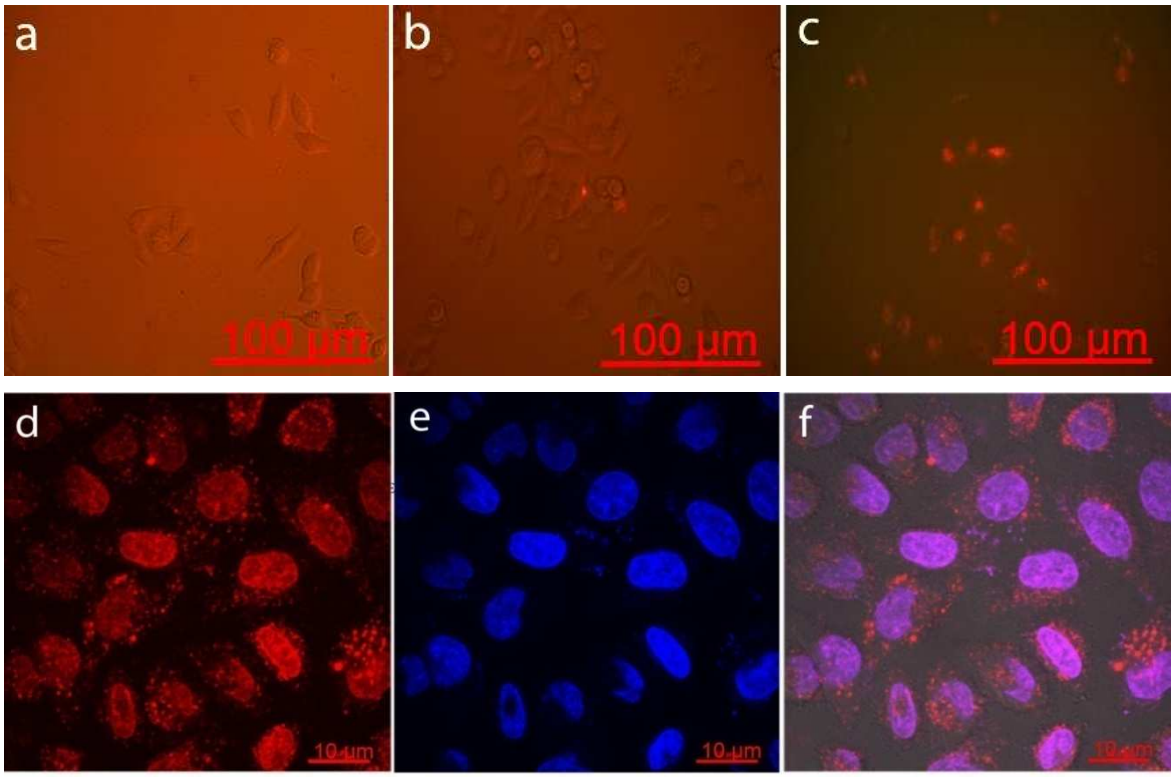

Figure 6. (a) Representative cells in group A (without QD and EGF). There is no red fluorescence. (b) Representative cells in group B (with only QD). Only weak fluorescence could be observed within several cells. (c) Representative cells in group C (with QD and EGF). Obvious fluorescence was observed in almost every cell; with red fluorescence gathered in the nucleus. With the exception of picture (c), all pictures were taken with a combination of bright field and fluorescence field using an Olympus IX71 fluorescence microscope. The exposure time was 300ms, and the magnification is 400×. (d) Locations of the quantum dots. (e) The red fluorescence located at the nucleus was stained with hochst33342. (f) Photo overlay of (d) and (e). Photos (d), (e) and (f) were taken with a Nikon A1RSi confocal fluorescence microscope.

To further confirm that the probes were indeed intracellular, they were also observed using a transmission electron microscopy. The cells of the test group were incubated with the probe. The control group was pure cells without a probe. Details of sample preparation have already been described [38]. We can clearly see that the nanoparticles were intracellular in Figure7a. However, most of the nanogolds were separated from the

QDs. It probably resulted from the effect of sectioning. There are no nanoparticles in control group cells (Figure 7b).

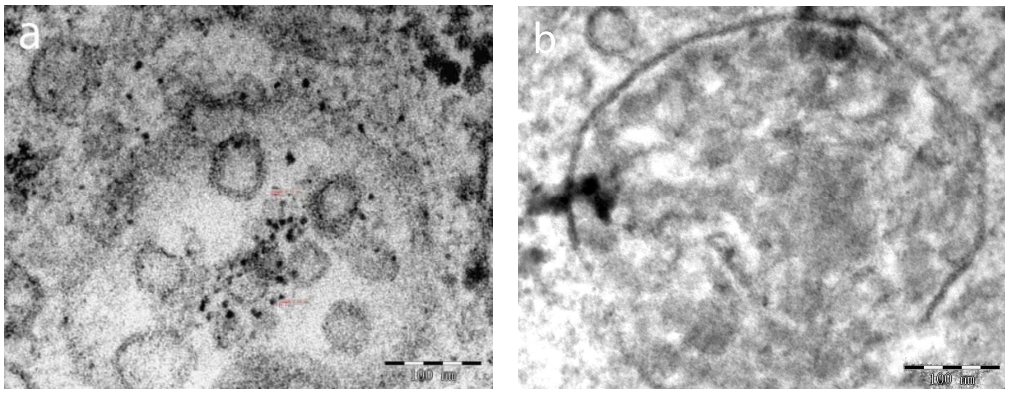

Figure 7. TEM images of a cell section. Intracellular nanoparticles conjugates observed by TEM. (a)Significant accumulation of nanoparticles (QDs). (b) HeLa cells without incubation with a probe.

3.4 Cell Induction and Detecting Caspase-3 Activity

We induced the apoptosis of HeLa cells with a combination of TNF-α and AcD according to the protocol in the previous section on cell induction. When cells were treated with TNF-α (20 ng/ml), AcD (0.2 μg/ml) was included in the medium to block the NF-kB mediated transcription of cyto protective TNF-α induced genes.[34]

After induction for 12hours, we detected the activity of caspase-3 in cells using the reagent kit purchased from Biovision and Biotium. According to the protocol, we separated cells into groups A(induced and then added substrate), B(induced and added inhibitor, then added substrate) and C(without induction but added substrate). Group A was induced without adding inhibitor. In group B, before adding the TNF-α and AcD, AC-DEVD-CHO and Z-VAD-FMK were added as a caspase inhibitor. Group C contained cells without induction.

Next, we added caspase-3 probes into the three groups and incubated them in a humidified atmosphere of 5% (vol/vol) CO_2 and 95% air (vol/vol) at 37 °C for 45min. Afterwards, the three groups were observed under the fluorescence microscope (Figure 8). Group A (group induced without inhibitor) is shown in Figure 8a, and 50% of the cells had shrunk. The picture shows the shrunken cells which are stained with the green fluorescence. It conforms to the fact that the caspase-3 would be activated when apoptosis occurs. In group B (Figure 8(b)), the ratio of the stained cell is about 10%, lower than group A (50% ratio). It can be explained by the inhibition of caspase-3 activity, and could hinder cell apoptosis. Figure 8(c) shows that the ratio of stained cells in group C was about 1%, and almost all non-stained cells were in good shape.

The conclusion from the assays was that after cells were induced by TNF-α and AcD, the caspase-3 was activated, and the shape of the corresponding cells shrank. A caspase-3 inhibitor could reduce their occurrence probability.

(a) Fluorescence field + Bright field Bright field

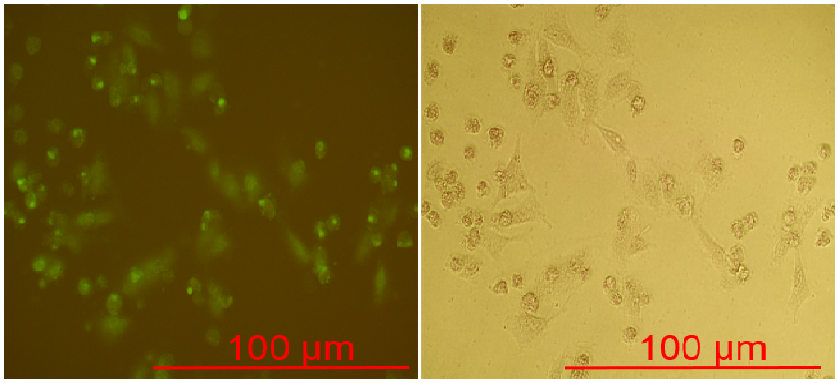

(b) Fluorescence field + Bright field Bright field

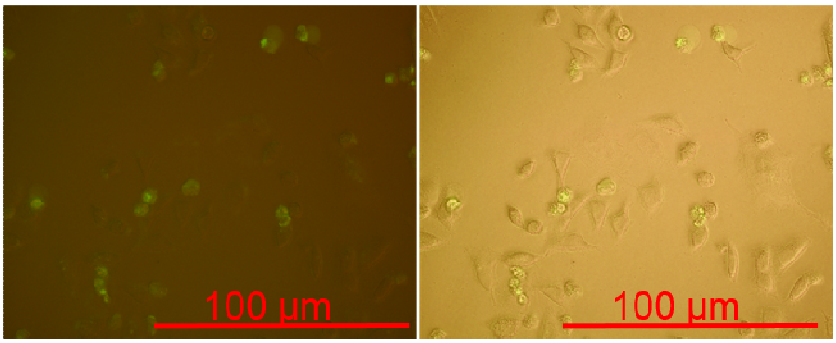

(c) Fluorescence field + Bright field Bright field

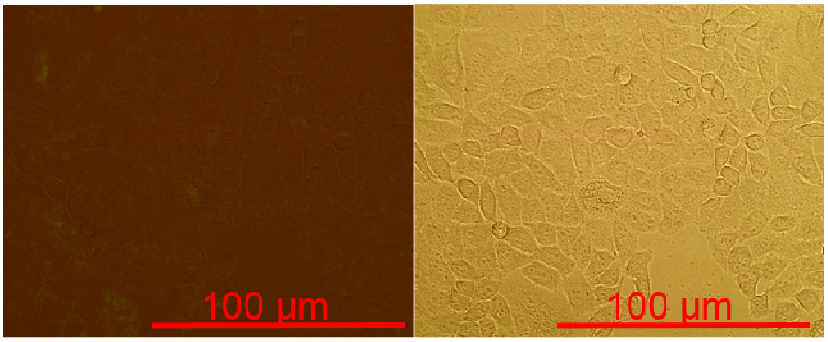

Figure 8. Characterization of the activity of caspase-3 in living HeLa cells by the reagent kit. (a) Induced and then added substrate. (b) Induced and added an inhibitor, then added substrate. (c) Without induction but added substrate. Photos were taken under combination of bright field and fluorescence field with an Olympus IX71 fluorescence microscope. Exposure time was 400ms, with 400× magnification.

3.5 Detecting Caspase-3 Activity in Live Cells via Synthesized Probes

HeLa and HL-60 cells were seeded in a 96-well micro plate filled with 100μl completed culture medium, and separated into groups A, B and C. At 60%-70% confluency, we transfected the probes (0.4μl, 1μM) into each well of the three groups according to the protocol described in "Experiment" section. Group A was then induced without adding inhibitor. In group B, before adding the TNF-α and AcD, AC-DEVD-CHO and Z-VAD-FMK were added as the caspase inhibitor. Group C contained cells without induction.

Twelve hours later, the three groups were observed under the fluorescence microscope. The results are shown in Figure 9 are similar to Figure 8. The induction time in Figure 8 was the same as that in Figure 9, which was 12 hours. In Figure 9(a) (group A), nearly half of the cells shrank. The shrunken cells are stained with the red fluorescence. The red fluorescence was gathered at the cell nucleus. It confirms to the fact that the EGF could carry the QD into the nucleus. In group B, the ratio of stained cell is about 10%. It is lower than that of group A (40%). Therefore, inhibiting caspase-3 activity could hinder the apoptosis of the cells. From Figure 9(c), we can deduce that the ratio of stained cells in group C was about 4%, and almost all the cells without clear fluorescence were in good shape.

(a) Induced

Fluorescence field + Bright field Bright field

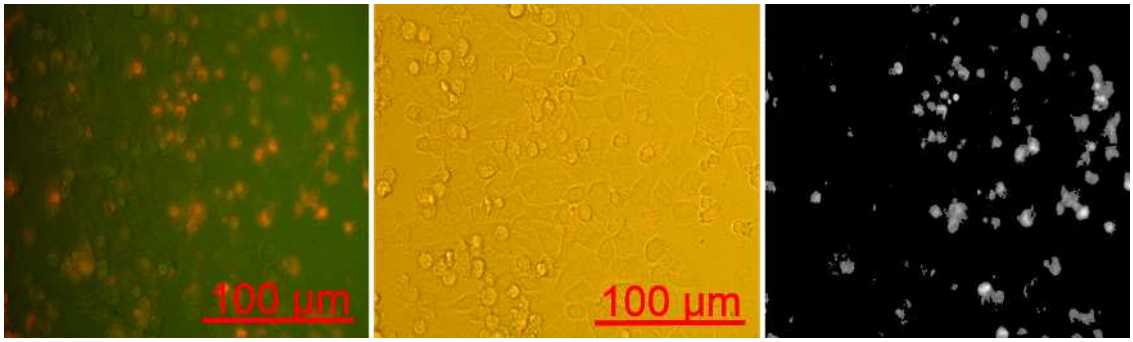

(b) Induced + inhibitor

Fluorescence field + Bright field Bright field

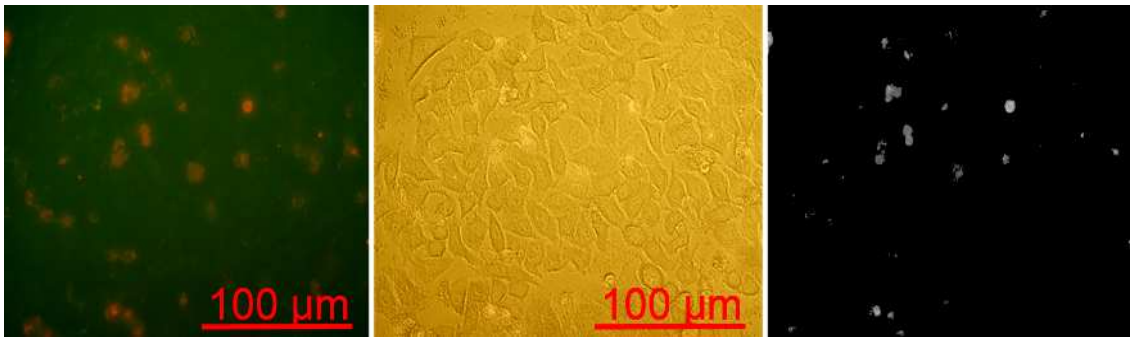

(c) No induction

Fluorescence field + Bright field Bright field

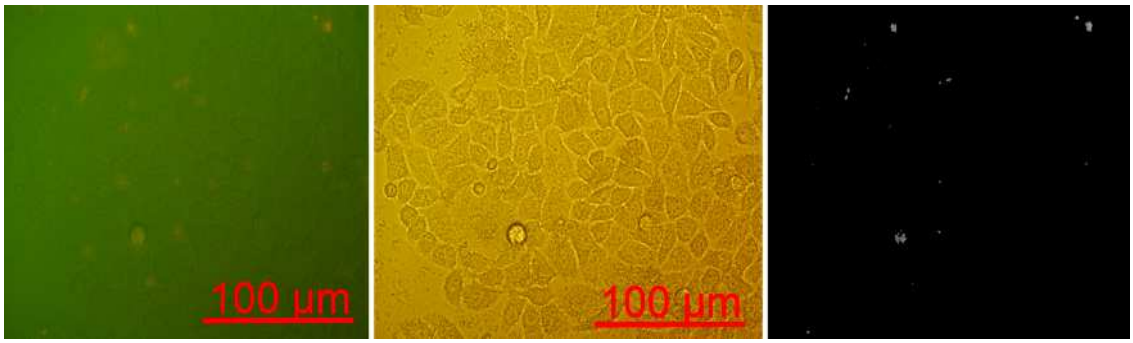

Figure 9. Characterization of the activity of caspase-3 in living HeLa cells by the probes. (a) Induced. (b) Induced with added inhibitor. (c) No induction.

We characterized the activity of caspase-3 by the product of the mean relative red fluorescence intensity

(MRRFI) in the cells and the ratio of cells with clear fluorescence to the total. First, we extracted the red channel of the image. Second, the background fluorescence of the image was erased and we targeted areas where the value of the color was higher than the threshold set. It is shown on the right of Figure 9. Third, we calculated the average of the color value in all areas, namely the mean relative red fluorescence intensity (Table 1). Then, we counted the ratio of cells with clear fluorescence to the total. Table 1 shows both the MRRFI and the ratio. Finally, the relative activity of caspase-3 was reflected by the relative fluorescence value, which is the product of the MRRFI and the ratio, namely Relative fluorescence value = MRRFI × Ratio .The result is shown in Figure 10.

Table 1 Calculation of the Activity of Caspase-3

Group No.	A	B	C
MRRFI	0.4736	0.4773	0.4373
Ratio (%)	40	10	4

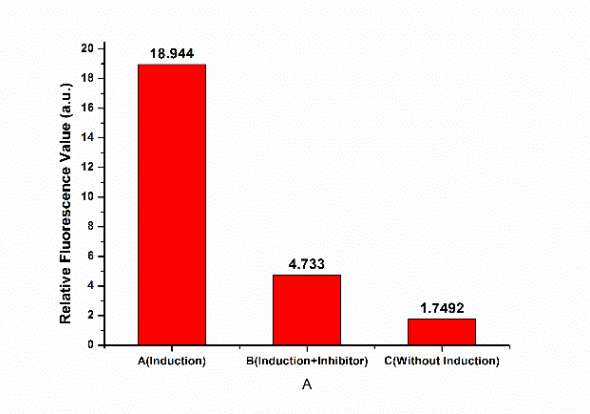

Figure 10. The relative fluorescence values of three groups.

3.6 Contrasting Assay: Photobleaching Resistance of QD and Alex488

When the relative fluorescence is used to characterize the activity of caspase-3, the decay of probe fluorescence during the observation should be considered, especially when the fluorescence signal must be collected in short intervals. However, traditional dyes bleach easily, and are unable to withstand the longtime exposure of excitation. As a result, truly real-time detection of proteases activity could not be achieved by the fluorescence-based probes composed of traditional dyes. Fortunately, QDs can overcome this problem and achieve real-time detection because of their strong photobleaching resistance. We conducted the assays to confirm this (Figure 11).

The cells were separated into groups A and B, and then the cells of group A were labeled with QD605, and group B with Streptavidin Alexa Fluor® 488 (SA-Alex488). Then we randomly selected a region and excited it continuously. At the same time, photos were taken at certain time point (Figure 11). From (a), we can see that the STR-488 faded quickly when exposed to excitation by laser. Just 0.5min later, the fluorescence intensity of STR-488 reduced obviously, and the fluorescence of STR-488 almost disappeared after being excited for 1 minute.

QD605 was quite different, which can be seen from the series of pictures (b). After excitation for 2 minutes, the red fluorescence of QD605 became clearer rather than faded, because of the decrease in background noise. Moreover, 6 minutes later, the probes' fluorescence intensity within the cells was almost unchanged. Actually, QDs are able to weather the excitation of a laser source for hours or even days[30,39]. The conclusion is that the

probe based on QD is able to meet the requirements of prolonged protease activity monitoring in living cells, which could not be achieved by conventional dye or fluorescent proteins.

(a)

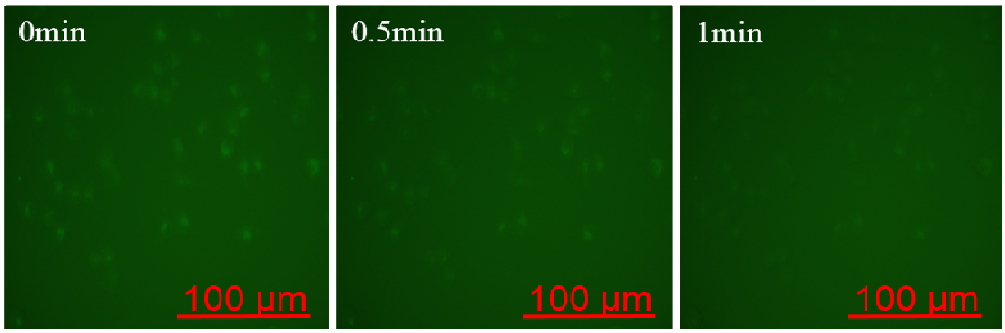

(b)

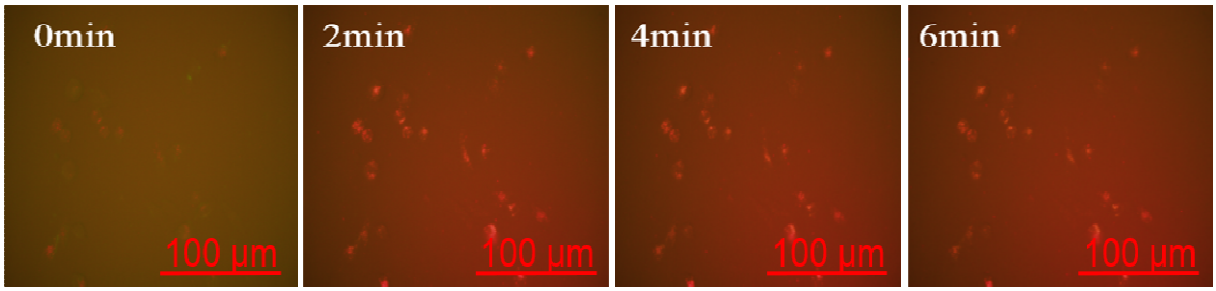

(c)

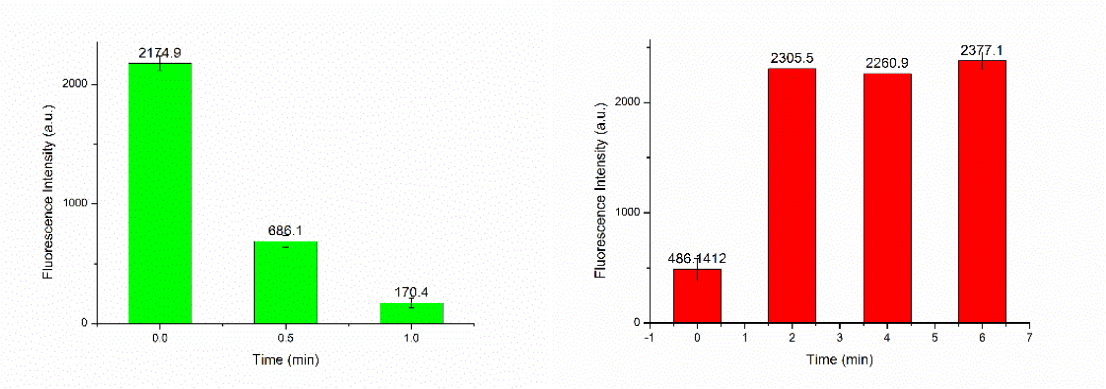

Figure 11. Changes in fluorescence intensity after exposure under an excitation light. (a) Fluorescence intensity changes of Alexa Fluor® 488. (b) Fluorescence intensity changes of QD605. (c) Quantification of fluorescence intensity changes.

As stated above, the long-term monitoring almost totally depends on the photobleaching resistance of fluorescence component contained in the probe. Therefore, conventional dye is not applicable to long-term continuously monitor the alteration of caspase-3 activities. Further experiments were taken to support the statement that one major advantage of this QD-based probe is long-term monitoring of caspase-3 activity,

We synthesized another kind of probe by replacing the SA-QD605 with SA-Alex488, and then we monitored the activity of caspase-3 using two kinds of probes. When the fluorescence of the cells were detected one time per hour and in each time the excitation lasted 3 seconds to complete the image acquisition, the results of caspase-3 characteristics were similar. As shown in (a) and (b) of figure 12, the fluorescence intensity of both groups increased. The difference between the results could be attributed to the difference in steric hindrance and photobleaching resistance.

However, continuous monitoring the activity of capase-3 over several minutes is impossible with conventional dyes as they were bleached quickly. As shown in (c) and (d) of Figure 12, after excitation for 10 minutes, the red fluorescence of the probes based on QD605 was almost unchanged. However, the green fluorescence of the probes based on Alexa Fluor® 488 faded quickly.

(a)

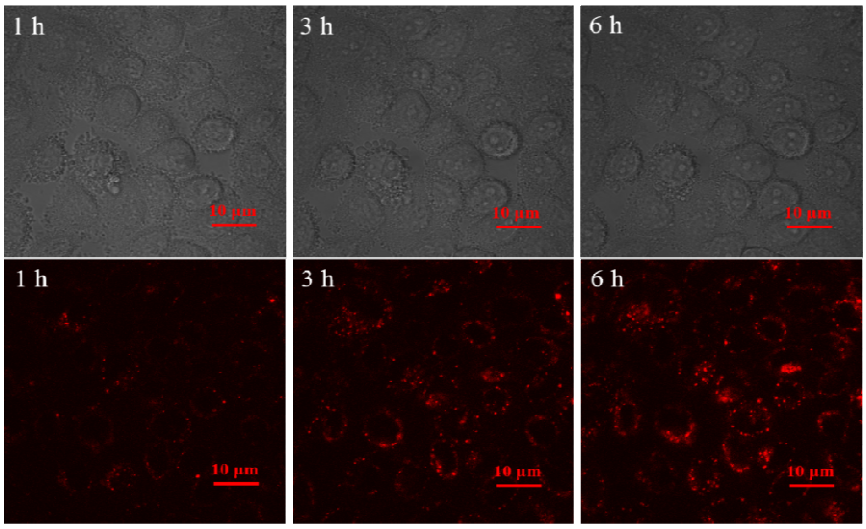

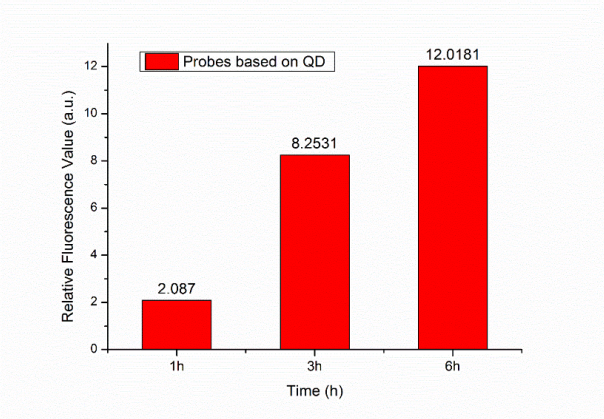

(b)

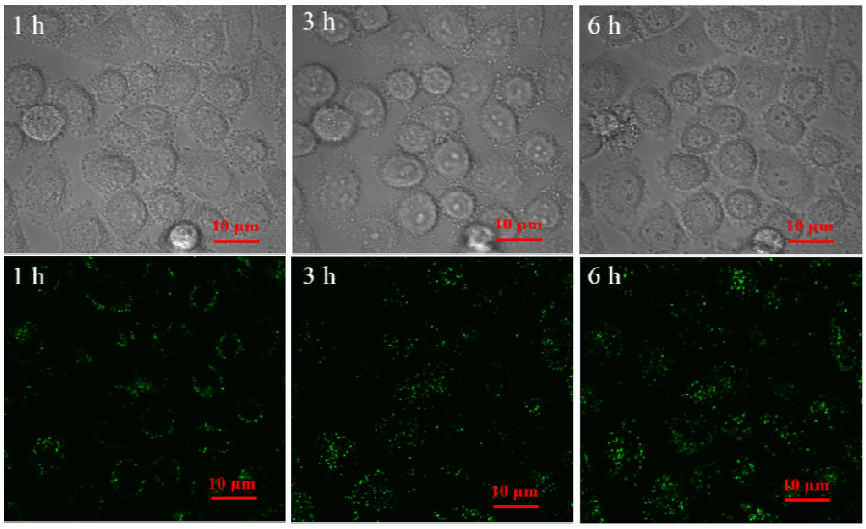

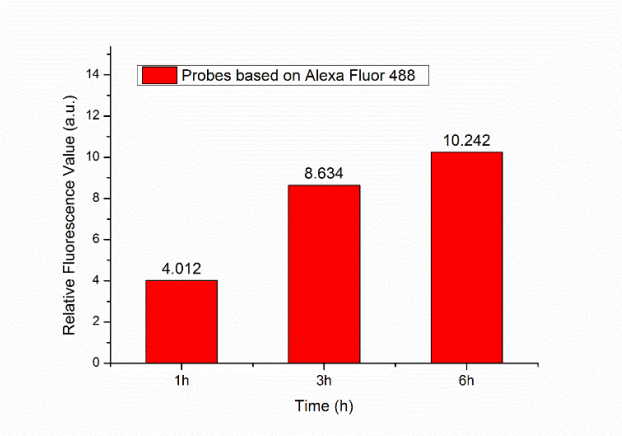

(c)

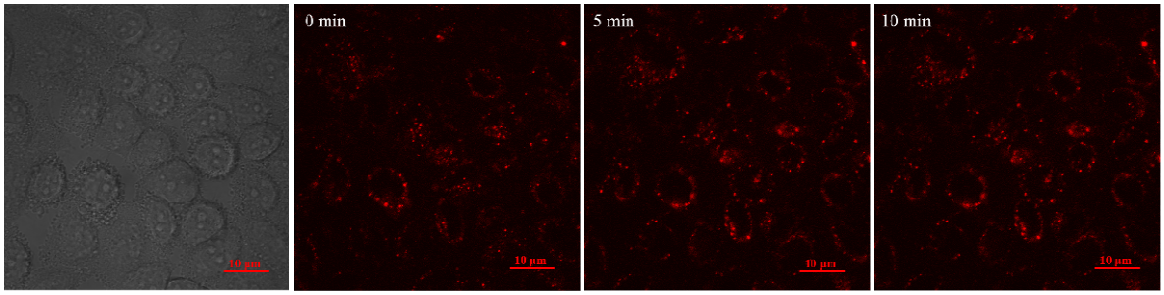

(d)

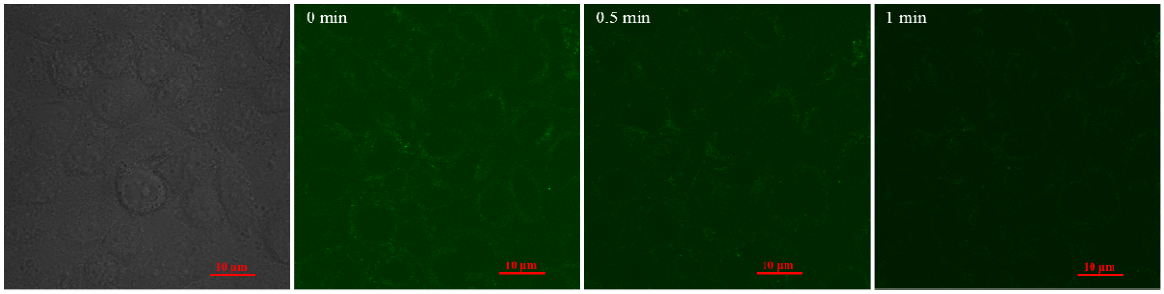

Figure 12. Time series of cells images. (a)The change of fluorescence intensity within cells and the shape of cells, which were transfected with probes based on QD. (b)The change of fluorescence intensity within cells and the shape of cells, which were transfected with probes based on Alexa Fluor® 488. (c)Fluorescence intensity changes of probes based on QD. (d)Fluorescence intensity changes of probes based on Alexa Fluor® 488.

4. Conclusions

In this study, based on QD, nanogold and EGF, we developed a unique probe which can be used to detect caspase-3 activity in real-time. Due to the minimum fluorescence overlapping and the strong photobleaching resistance of QDs, the strong photo quenching efficiency of nanogolds, and the high EGF transfer efficiency, this probe can be employed to achieve prolonged real-time intracellular multiplex detection and to reveal the relations between proteases.

Because the emission spectrum of QD is much narrower than conventional dye or fluorescent protein, the probe based on QD is also the best candidate for the parallel detection of proteases in living cells. This can be

achieved by replacing the specific substrate peptide and QD. One kind of protease corresponds to one kind of specific substrate peptide and QD with a specific different color. The probe we developed has the potential to illustrate the mechanism of proteases by exerting their function, and may serve as a model for strategies aimed at monitoring the activity of other intracellular proteases. Moreover, this kind of probe is not limited to detecting the activity of proteases. It can also be used to detect other types of enzymes like DNA, and even certain kinds of molecules.

Acknowledgements

This work is supported by the National Natural Science Foundation of China (No. 61071002), National Program for Significant Scientific Instruments Development of China (No. 2011YQ030134), the Funds for State Key Laboratory of China, the Scientific Research Foundation for Returned Overseas Chinese Scholars and the Fund for Beijing Laboratory of Biomedical Detection Technology and Instrument. We also thank Professor Yinye Wang of Beijing University for the cell supports.

References

[1] D. R. Green, B. Levine, To be or not to be? How selective autophagy and cell death govern cell fate, Cell, vol. 157, no. 1, pp. 65-75, 2014.

[2] Y. X. Wu, D. Xing, S. M. Luo et al., Detection of caspase-3 activation in single cells by fluorescence resonance energy transfer during photodynarnic therapy induced apoptosis, Cancer Letters, vol. 235, no. 2, pp. 239-247, Apr 28, 2006.

[3] P. Broz, D. M. Monack, Newly described pattern recognition receptors team up against intracellular pathogens, Nature Reviews Immunology, vol. 13, pp. 551-565, 2013.

[4] Y. Aachoui, I. A. Leaf, J. A. Hagar, M. F. Fontana, Caspase-11 protects against bacteria that escape the vacuole, Science, vol. 339, no. 6122, pp. 975-978, 2013.

[5] J. Suzuki, D. P. Denning, E. Imanishi, H. R. Horvitz, S. Nagata, Xk-Related Protein 8 and CED-8 Promote Phosphatidylserine Exposure in Apoptotic Cells, Science, vol. 341, no. 6144, pp. 403-406, 2013.

[6] S. Lu, Y. Wang, H. Huang et al., Quantitative FRET imaging to visualize the invasiveness of live breast cancer cells, PLoS One, vol. 8, no. 3, pp. e58569, 2013.

[7] A. Banerjee, A. Sahana, S. Lohar, B. Sarkar, S. K. Mukhopadhyay, D. Das, A FRET operated sensor for intracellular pH mapping: strategically improved efficiency on moving from an anthracene to a naphthalene derivative, RSC Advances, vol. 3, pp.14397-14405, 2013.

[8] Rabeka Alam, Joshua Zylstra, Danielle M. Fontaine, Bruce R. Branchini, Mathew M. Maye, Novel multistep BRET-FRET energy transfer using nanoconjugates of firefly proteins, quantum dots, and red fluorescent proteins, Nanoscale, vol.5, pp. 5303-5306, 2013.

[9] D. D. Sua, C. L. Teoha, S. Sahua, R. K. Dasa, Y. T. Chang, Live cells imaging using a turn-on FRET-based BODIPY probe for biothiols, Biomaterials, vol. 35, no. 23, pp. 6078 – 6085, 2014.

[10] H. Z. Zhang, S. Kasibhatla, J. Guastella et al., N-Ac-DEVD-N '-(polyfluorobenzoyl)-R110: Novel cell-permeable fluorogenic caspase substrates for the detection of caspase activity and apoptosis, Bioconjugate Chemistry, vol. 14, no. 2, pp. 458-463, Mar-Apr, 2003.

[11] P. A. Amstad, G. Yu, G. L. Johnson et al., Detection of caspase activation in situ by fluorochrome-labeled caspase inhibitors, Biotechniques, vol. 31, no. 3, pp. 608-+, Sep, 2001.

[12] N. Chen, Y. Huang, L. Yang et al., Designing caspase-3 sensors for imaging of apoptosis in living cells, Chemistry, vol. 15, no. 37, pp. 9311-4, Sep 21, 2009.

[13] W. Gao, L. Ji, L. Li et al., Bifunctional combined Au-Fe2O3 nanoparticles for induction of cancer cell-specific apoptosis and real-time imaging, Biomaterials, vol. 33, no. 14, pp. 3710-3718, 2012.

[14] B. R. Knudsen, M. L. Jepsen, and Y.-P. Ho, Quantum dot-based nanosensors for diagnosis via enzyme activity measurement, Expert Review of Molecular Diagnostics, vol. 13, no. 4, pp. 367-375, 2013.

[15] Y.-P. Kim, Y.-H. Oh, E. Oh et al., Energy transfer-based multiplexed assay of proteases by using gold nanoparticle and quantum dot conjugates on a surface, Analytical Chemistry, vol. 80, no. 12, pp. 4634-4641, 2008.

[16] X. Wang, Y. Q. Xia, Y. Y. Liu et al., Dual-Luminophore-Labeled Gold Nanoparticles with Completely Resolved Emission for the Simultaneous Imaging of MMP-2 and MMP-7 in Living Cells under Single Wavelength Excitation, Chemistry-a European Journal, vol. 18, no. 23, pp. 7189-7195, 2012.

[17] S. Y. Park, S. M. Lee, G. B. Kim et al., Gold nanoparticle-based fluorescence quenching via metal coordination for assaying protease activity, Gold Bulletin, vol. 45, no. 4, pp. 213-219, 2012.

[18] Y. Choi, Y. Cho, M. Kim et al., Fluorogenic Quantum Dot-Gold Nanoparticle Assembly for Beta Secretase Inhibitor Screening in Live Cell, Anal Chem, 2012.

[19] L. Yao, J. Daniels, A. Moshnikova et al., pHLIP peptide targets nanogold particles to tumors, Proceedings of the National Academy of Sciences, vol. 110, no. 2, pp. 465-470, January 8, 2013, 2013.

[20] S.-i. Sato, Y. Kwon, S. Kamisuki et al., Polyproline-rod approach to isolating protein targets of bioactive small molecules: Isolation of a new target of indomethacin, Journal of the American Chemical Society, vol. 129, no. 4, pp. 873-880, 2007.

[21] J. K. Jaiswal, H. Mattoussi, J. M. Mauro et al., Long-term multiple color imaging of live cells using quantum dot bioconjugates, Nature Biotechnology, vol. 21, no. 1, pp. 47-51, 2003.

[22] H. Cen, F. Mao, I. Aronchik et al., DEVD-NucView488: a novel class of enzyme substrates for real-time detection of caspase-3 activity in live cells, FASEB Journal, vol. 22, no. 7, pp. 2243-2252, 2008.

[23] E. Chang, J. S. Miller, J. T. Sun et al., Protease-activated quantum dot probes, Biochemical and Biophysical Research Communications, vol. 334, no. 4, pp. 1317-1321, 2005.

[24] T. Pons, I. L. Medintz, K. E. Sapsford et al., On the quenching of semiconductor quantum dot photoluminescence by proximal gold nanoparticles, Nano Letters, vol. 7, no. 10, pp. 3157-3164, 2007.

[25] C. S. Yun, A. Javier, T. Jennings et al., Nanometal surface energy transfer in optical rulers, breaking the FRET barrier, Journal of the American Chemical Society, vol. 127, no. 9, pp. 3115-3119, 2005.

[26] E. Dulkeith, A. C. Morteani, T. Niedereichholz et al., Fluorescence Quenching of Dye Molecules near Gold Nanoparticles: Radiative and Nonradiative Effects, Physical Review Letters, vol. 89, no. 20, pp. 203002, 2002.

[27] D. S. Lidke, P. Nagy, R. Heintzmann et al., Quantum dot ligands provide new insights into erbB/HER receptor-mediated signal transduction, Nature Biotechnology, vol. 22, no. 2, pp. 198-203, 2004.

[28] H. Lee, T. H. Kim, and T. G. Park, A receptor-mediated gene delivery system using streptavidin and biotin-derivatized, pegylated epidermal growth factor, Journal of Controlled Release, vol. 83, no. 1, pp. 109-119, 2002.

[29] P. Diagaradjane, J. M. Orenstein-Cardona, N. E. Colon-Casasnovas et al., Imaging epidermal growth factor receptor expression in vivo, Clin Cancer Res, vol. 14, no. 3, pp. 731-41, 2008.

[30] C. L. Arteaga, Epidermal growth factor receptor dependence in human tumors: More than just

expression?, Oncologist, vol. 7, pp. 31-39, 2002.

[31] J. Liu, and Y. Lu, Preparation of aptamer-linked gold nanoparticle purple aggregates for colorimetric sensing of analytes, Nat. Protocols, vol. 1, no. 1, pp. 246-252, 2006.

[32] D. H. Ren, Y. Q. Xia, Z. You, Multiplexed living cells staining with quantum dot bio-probes for multiplexed detection of single-cell array, Journal of biomedical optics, vol. 18, no. 9, pp.096005(1-9), 2013.

[33] S. B. Lowe, J. A. G. Dick, B. E. Cohen et al., Multiplex Sensing of Protease and Kinase Enzyme Activity via Orthogonal Coupling of Quantum Dot Peptide Conjugates, ACS Nano, vol. 6, no. 1, pp. 851-857, 2012.

[34] M. E. Guicciardi, J. Deussing, H. Miyoshi et al., Cathepsin B contributes to TNF-alpha-mediated hepatocyte apoptosis by promoting mitochondrial release of cytochrome c, J Clin Invest, vol. 106, no. 9, pp. 1127-37, 2000.

[35] D. Fabian, S. Juhas, G. Il'kova et al., Dose- and time-dependent effects of TNFalpha and actinomycin D on cell death incidence and embryo growth in mouse blastocysts, Zygote, vol. 15, no. 3, pp. 241-9, 2007.

[36] S. Hakoda, H. Ishikura, N. Takeyama et al., Tumor necrosis factor-alpha plus actinomycin D-induced apoptosis of L929 cells is prevented by nitric oxide, Surg Today, vol. 29, no. 10, pp. 1059-67, 1999.

[37] E. Oh, M. Y. Hong, D. Lee et al., Inhibition assay of biomolecules based on fluorescence resonance energy transfer (FRET) between quantum dots and gold nanoparticles, Journal of the American Chemical Society, vol. 127, no. 10, pp. 3270-3271, 2005.

[38] C. D. Dekiwadia, A. C. Lawrie, and J. V. Fecondo, Peptide-mediated cell penetration and targeted delivery of gold nanoparticles into lysosomes, J Pept Sci, vol. 18, no. 8, pp. 527-34, 2012.

[39] F. Chen, and D. Gerion, Fluorescent CdSe/ZnS Nanocrystal−Peptide Conjugates for Long-term, Nontoxic Imaging and Nuclear Targeting in Living Cells, Nano Letters, vol. 4, no. 10, pp. 1827-1832, 2004.